

## SYNTHESIS AND CHARACTERIZATION OF ZnO/FLY ASH COMPOSITE WITH HIGHLY PHOTOCATALYTIC ACTIVITY USING A HYDROTHERMAL PROCESS

H. J. KIM<sup>a,b</sup>, C. S. KIM<sup>a, b\*</sup>

<sup>a</sup>*Department of Bio-nanosystem Engineering, Chonbuk National University, Jeonju 561-756, Republic of Korea*

<sup>b</sup>*Division of Mechanical Design Engineering, Chonbuk National University, Jeonju 561-756, Republic of Korea*

This study reports a facile strategy to fabricate unique clustered ZnO-doped fly ash particle (FAP) composite material with highly effective photocatalytic activity using a hydrothermal process. The photocatalytic efficiency was evaluated based on the photodegradation of methylene blue (MB). The characterization of the ZnO/FAP composite was investigated using several analytical methods including field emission scanning electron microscopy (FE-SEM), energy dispersive spectroscopy (EDS), transmission electron microscopy (TEM), X-ray diffraction (XRD), Fourier transform infrared spectroscopy (FT-IR), and photoluminescence spectroscopy (PL). Furthermore, an increase in specific surface area measurement (Brunauer–Emmett–Teller method [BET]) of the ZnO/FAP composite was produced to greatly enhance the photocatalytic property compared to that of ZnO. The results showed that ZnO flowers were effectively incorporated onto the surface FAPs with unique cluster-shaped aspects. Therefore, the as-synthesized composite has potential as a photocatalytic filler material in pollution applications as an economically and environmentally friendly photocatalyst.

(Received June 27, 2014; Accepted August 8, 2014)

*Keywords:* ZnO, Composite; Fly ash; Photocatalyst; Hydrothermal

### 1. Introduction

Recently, heterogeneous photocatalysis has emerged as a viable and effective method for the removal of harmful environmental elements using organic and inorganic materials [1, 2]. Among these materials, use of oxide-based catalysis using compounds such as TiO<sub>2</sub> and ZnO has greatly increased. A suspension of TiO<sub>2</sub> has photocatalytic degradation ability [3], immobilized TiO<sub>2</sub> photocatalytic systems are commonly used for the photodegradation of organic materials [4], and ZnO incorporated with inorganic materials can be enhanced to obtain more effective photocatalysis [5]. Thus, it is believed that ZnO has more energetic activation than TiO<sub>2</sub> due to its superior dispersion during fabrication. Using an inexpensive matrix and a facile method, this study aimed to produce effective photocatalytic results with inorganic materials. ZnO as a catalyst has attracted much attention not only for composite conversion, but also because of it is an inexpensive and valuable material for use in semiconductors due to its direct bandgap ( $E_g=3.37$  eV) and high binding energy (60 mV) [6-8]. More effective semiconductor photocatalysis to produce desired physicochemical characteristics has been the aim of many research efforts. ZnO has been reported to have distinctive catalytic and photochemical properties [9-11] and can be functionally activated at lower temperatures under ultraviolet (UV) irradiation [12-14]. Moreover, nanoparticles of ZnO have demonstrated desirable effects due to their strong dispersion and large

---

\* Corresponding authors: chskim@jbnu.ac.kr

total surface area [15, 16]. However, ZnO is unstable in alkali conditions and has a tendency for self-aggregation [17], which results in considerably reduced photocatalytic performance. Thus, these properties of scattering and aggregating can produce a stronger catalytic effect through incorporation with adsorbent materials such as fly ash particles (FAPs) [18] or activated carbon [19]. FAPs, inorganic residue generated in the combustion of coal, consist of fine powdery particles having a spherical shape and substantial granular components of silicon dioxide ( $\text{SiO}_2$ ), alumina ( $\text{Al}_2\text{O}_3$ ), calcium oxide (CaO), magnesium (MgO), and titanium ( $\text{TiO}_2$ ) [20]. At present, FAPs are used as an additive in cement manufacture [21-23], although their use is limited by their negative environmental impact. Previous studies have focused on development of effective ways to convert fly ash (FA) into composite materials by chemical treatment [24, 25]. Thus, FAPs that have nontoxic and excellent absorbance properties have been used to create functional substrates and to modify catalytic materials in order to reduce pollutants. Additionally, composite material with FAPs has an enhanced mechanical property and a higher specific surface area that produce effective performance for physicochemical treatment [4]. The incorporation of ZnO on the surface of FAPs is generally performed to enhance the photocatalysis of a pollutant solution. Therefore, we analyzed the additive effects of FAPs on the photocatalytic properties of ZnO. FAP-incorporated ZnO is expected to be an effective photocatalyst to reduce harmful pollutants from the environment [1, 26]. Some such approaches to reduce toxins include the use of activated solid loading in solvent-based system; Yeole *et al.* reported an effective method to protect an effective corrosion inhibitor by coating ZnO on the surface of FA [4]. The application of a functional composite that interacts with inorganic materials can be effectively utilized in a polymeric matrix [27]. Although many researchers have attempted to produce ZnO/FA composite, to the best of our knowledge, the synthesis of ZnO/FA composites using a hydrothermal process has not been reported. Here, we hydrothermally synthesized uniquely shaped ZnO flowers in a novel composite incorporating FAPs in order to produce a strong photocatalytic effect. This facile, cost-effective method was designed to remove pollutant components.

## **2. Experimental**

### **2.1. Materials**

FAPs were obtained from Won Engineering Company, Ltd. (Gunsan, Korea); they were ball-milled for 12 h using 3-mm zirconia balls and then filtered. Zinc nitrate hexahydrate, bis-hexamethylene trimine, and methylene blue (MB) were used without any further purification.

### **2.2. Preparation of photocatalysts**

Pristine ZnO flowers were prepared by mixing 0.5 g of bis-hexamethylene trimine in 40 ml distilled water and 0.75 g zinc nitrate hexahydrate in 40 ml distilled water. The slurry of mixed solution was vigorously stirred for an additional 30 min and then placed in a Teflon crucible inside the autoclave to activate the hydrothermal process. Different amounts of FAPs (20, 50, and 100 mg) were dissolved in 20 mL of distilled water and ultrasonicated in a bath sonicator for 30 min. These solutions were then added to 0.5 g of bis-hexamethylene trimine in 30 ml distilled water and 0.75 g zinc nitrate hexahydrate in 30 ml distilled water. The slurries were maintained at 120°C for 1.5 h and were named as follows: NM-0, NM-1, NM-2, and NM-3 which refer to 0, 20, 50, and 100 mg FAPs, respectively.

### **2.3. Characterization**

The surface morphologies of as-synthesized pristine ZnO and ZnO/FAPs samples were observed using field-emission scanning electron microscopy (FE-SEM, S-7400, Hitachi, Japan). Elemental components of the samples were analyzed by energy dispersive spectroscopy (EDS)

connected to FE-SEM. X-ray diffraction (XRD) analysis was carried out by a Rigaku X-ray diffractometer (Cu K $\alpha$ ,  $\lambda = 1.54059 \text{ \AA}$ ) over Bragg angles ranging from 20 to 80°. Fourier-transform infrared (FTIR) spectra of the samples were produced using a Paragon 1000 spectrometer (Perkin Elmer), and photoluminescence (PL) spectra were produced using a Perkins Elmer instrument (LS55) at room temperature. To evaluate the photocatalytic activity of pristine ZnO and ZnO/FAPs samples, we measured the degradation of MB dye solution. The degradation was produced by subjecting bottles (dia. 50  $\times$  height 50 cm) containing the individual samples to ultraviolet light ( $\lambda=365 \text{ nm}$ ) at a distance of 5 cm. The dye solution (30 ml, 10 ppm concentration) and each 15 mg sample were stirred to assure suspension during measurement. The initial sample evaluation was conducted after 30 min of darkness, and all subsequent 1 ml samples were extracted in 30 min intervals for 180 min at room temperature. The samples were centrifuged at high speed in order to separate the residual catalyst, and the absorbance levels and wavelengths were measured using UV-visible spectrophotometry (UV-Vis) (HP 8453, Hewlett Packard, Germany). To determine the reliability of the experimental results, a few repeat measurements were performed. The degradation rate of MB was calculated by the following equation:

$$\text{Degradation efficiency (\%)} = \left(1 - \frac{C}{C_0}\right) \times 100$$

where  $C_0$  is the initial concentration of MB, and  $C$  is the concentration of MB after "t" minutes of UV irradiation. For the evaluation of recycling efficiency, the ZnO/FAPs composite was washed and used in a repeat experiment using the same process.

### 3. Results and discussion

ZnO particles incorporated with FAPs have been utilized as a photocatalyst for the photodegradation of harmful environmental pollutants. This use motivated our fabrication of uniquely shaped ZnO/FAPs composites using a hydrothermal process in order to achieve highly effective photocatalytic function. Figure 1 shows representative FE-SEM images with EDS spectra of pristine ZnO, raw FAPs, and the ZnO/FAPs composites. The FAPs are the fine particles in the figure and consisted of small spheres that are irregular, porous, and amorphous with sizes ranging from 0.1 to 100  $\mu\text{m}$  after ball-mill grinding (Fig. 1a). The EDS analysis of the ball-milled raw FA (NM-0) revealed elements consisting of the typical elements of O, Al, Si, Ti, and Ca. Different amounts (20, 50, and 100 mg) of well-dispersed FAPs in solution with bis-hexamethylene triamine and nitrate hexahydrate were prepared using a hydrothermal process to produce ZnO-doped FAP photocatalyst. The FE-SEM image of pristine ZnO in the mixture of bis-hexamethylene triamine and nitrate hexahydrate showed unique flower-shaped ZnO particles (inset of Fig. 1b), as similarly described in Pant *et al.* [15, 28]. These ZnO flowers were then incorporated in unique cluster shapes onto the surfaces of FAPs (Figs. 1c-d). The cluster shape (spherical) of the ZnO flowers of nano/micro sizes increase the total material surface area and produce strong photocatalytic effects. Compared to pristine ZnO flowers, ZnO/FAP composites clearly showed irregular clusters of ZnO flowers on the surfaces of FAPs. The formation of pristine ZnO particles (Fig. 1b) and their growth on FAPs was uniform without aggregation. However, the formation of large-scale ZnO/FAPs composites resulted in clustering with increasing FAP concentration in the hydrothermal solution (Figs. 2a-c). These results indicate better interaction between particles of composite molecules at higher concentration and incorporation of ZnO particles with increased FAP concentration. Figure 2a shows an FE-SEM image of NM-3 with ZnO on the surfaces of FAPs, resulting in clusters of differing sizes. EDS analysis showed that various elements found in FAPs (Fig. 1a) were also found in the ZnO/FAPs composite (Fig. 2a), confirming the presence of ZnO and FAPs in the composites. The FAPs had different shapes and were irregularly distributed within the matrix (Fig. 1a). As the amount of FAPs was increased in the solution, the sizes of the

clusters increased (Fig. 2c). Homogeneous dispersion was achieved in the mixtures with 50 mg and 100 mg of FAPs in ZnO solution, and the amount of added FAPs affected the photocatalytic performance to reduce the pollutants.

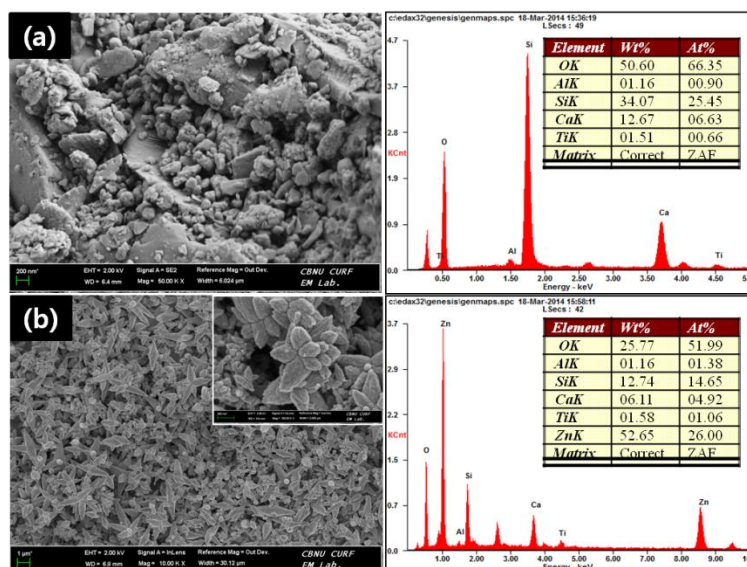


Fig. 1. FE-SEM images and the corresponding EDS of (a) raw FAPs, and (b) pristine ZnO.

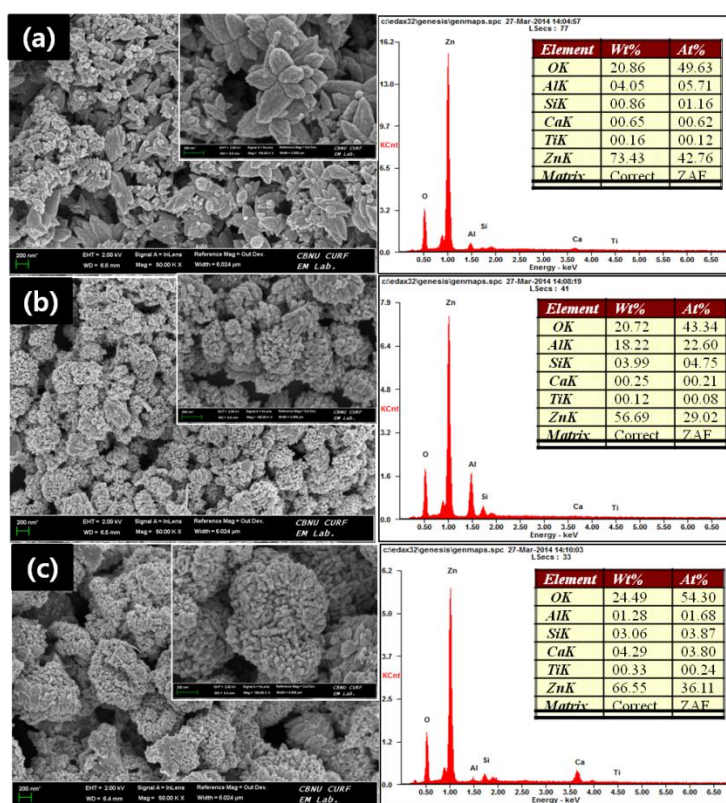


Fig. 2. FE-SEM images and the corresponding EDS of (a) ZnO/FAPs 20 mg, (b) ZnO/FAPs 50 mg, and (c) ZnO/FAPs 100 mg

To examine the morphology of ZnO/FAP composites, transmission electron microscopy (TEM) was utilized to analyze the crystalline and amorphous states. The structural aspect of as

prepared ZnO/FAP composite had a unique flower shape under low magnification and specific uniform shapes between layers under high magnification, as shown in Fig. 3.

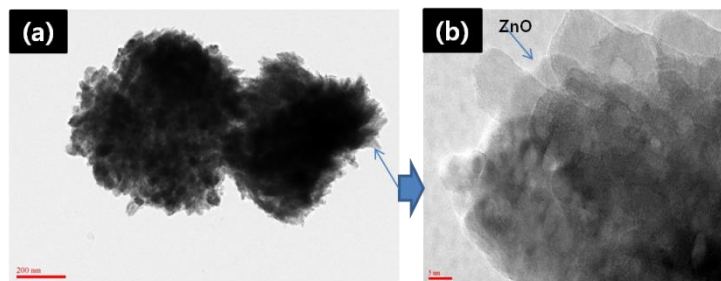


Fig. 3. TEM images of pristine ZnO flowers on the surface of FAPs

In order to investigate the interaction of ZnO and a FAP matrix, we performed Fourier transform infrared spectroscopy (FT-IR), XRD, and PL measurements. To analyze the elements of ZnO and FAPs, XRD patterns of pristine ZnO and the different samples were measured as shown in Fig. 4. The observed peaks were in agreement with those reported in Jiang *et al.* and Yeole *et al.* [4, 29]. The intensities of the peaks had a tendency to strongly increase with increased amount of FAPs in the composite, as shown in Figs. 4c-e. The many peaks of the composite indicate the presence of ZnO and FAPs, as many new peaks existed in the composite (Figs. 4c-e) compared to pristine ZnO (Fig. 4a). Figure 4 clearly illustrates peaks indicating the existence of mullite, quartz crystal, and ZnO [30]. The peaks of mullite are strong and correspond to crystallization; higher intensity peaks was produced with increased amount of FAPs in the composite.

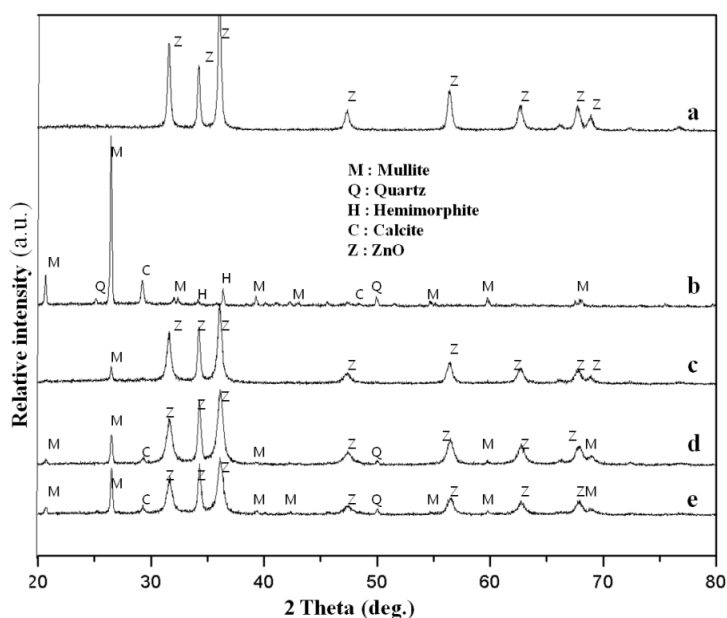


Fig. 4. XRD patterns of (a) pristine ZnO, (b) raw FAPs, (c) ZnO/FAPs 20 mg, (d) ZnO/FAPs 50 mg, and (e) ZnO/FAPs 100 mg

Additionally, the molecular structures of pristine ZnO and the composites were investigated by FT-IR, and their FT-IR spectra are shown in Fig. 5. The IR bands of ZnO were similar to those of our previous study [31]; however, new peaks at  $799\text{ cm}^{-1}$ ,  $855\text{ cm}^{-1}$ ,  $996\text{ cm}^{-1}$ , and  $2847\text{ cm}^{-1}$  (Si–O–Si bond bending vibration absorption) [30] were observed for the composites, especially at higher FAP concentrations, and are attributed to the presence of ZnO and

FAPs. Furthermore, the rightward peak shift in the composite was attributed to the interactions between ZnO and FAPs through hydrogen or dative bonds.

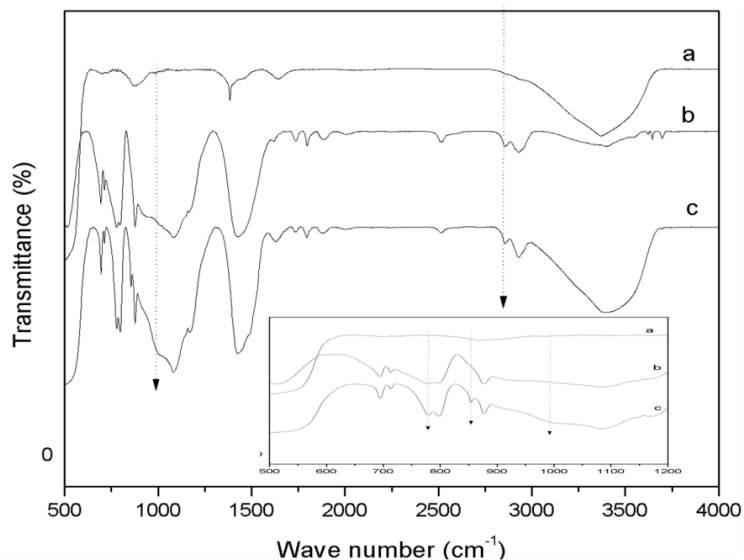


Fig. 5. FT-IR spectra of (a) pristine ZnO, (b) ZnO/FAPs 100 mg, and (c) raw FAPs.

*Inset shows the detailed spectra of lower wave numbers*

To further support the functions of ZnO/FAPs composite, PL spectra were measured for the different samples. The comparison curves of the pristine ZnO and ZnO/FAPs composites are shown in Fig. 5 and apparently indicated the degradation effects of ZnO on the FAP matrix.

The PL emission intensity is dominated by bond energy for the recombination of excited electrons and holes [32]. The results showed that pristine ZnO produced higher emission than ZnO/FAP composites due to the decreased recombination rate between ZnO and FAPs in the composite [32]. However, as reported in Yang *et al.* [33], the excited electrons of ZnO were transferred from the conduction band of ZnO into FAPs through reactive carriers in the ZnO/FAP composite and promoted the photodegradation of dyes. Furthermore, Fig. 6 shows a shift in the high intense peak of pristine ZnO from 374 nm to 417 nm in the composite, whereas a weak peak of pristine ZnO was observed at lower intensity at 446 nm. The intensity of pristine ZnO exhibited behavior typical of higher photocatalytic materials [28]. However, the composite showed a decreased value for this behavior. In the ZnO/FAPs composite, it was considered that the presence of ZnO/FAP heterojunctions may decrease the recombination rate, while the migrating movement of e-h is attributed to the enhancement of the photocatalytic effect that will motivate the occurrence of the redox process [34]. Accordingly, compared to pristine ZnO, the less intense peaks of the ZnO/FAP composite were related to the decreased recombination rate and the higher efficiency of the photocatalytic effects. These results confirm those of Pant *et al.* [15].

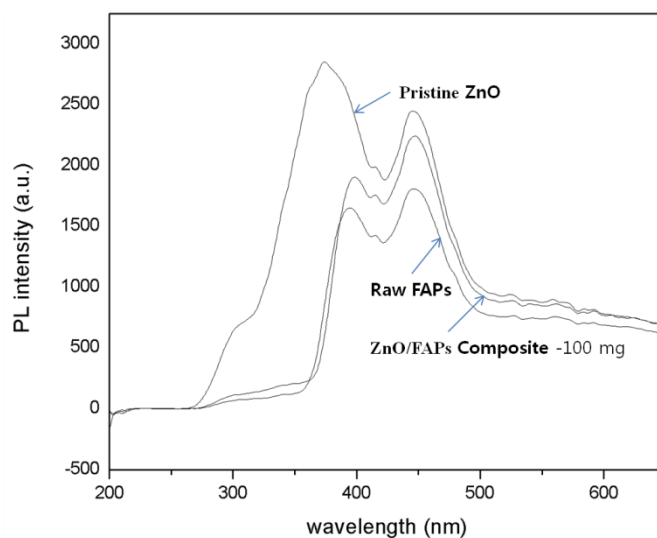


Fig. 6. PL spectra of (a) pristine ZnO, (b) ZnO/FAPs 100 mg, and (c) raw FAPs.

To analyze the photocatalytic performance, surface area measurements of the samples were required and were carried out for pristine ZnO, NM-0, NM-2, and NM-3 composites as indicated in Table 1. The photocatalytic effect of the ZnO-doped FAP matrix was greatly enhanced. A higher amount of FAPs produced increased diffusion of ZnO, which was induced to increase the total surface area of the composite and also to increase the photocatalytic property. The results were determined from nitrogen adsorption-desorption isotherms using the Brunauer–Emmett–Teller method (BET) and Langmuir equation, respectively. Compared to that of pristine ZnO and raw FAPs, the specific surface areas of ZnO/FAP composites were greatly increased through the use of a hydrothermal process. This increase resulted from the interactions between ZnO and FAPs to produce ZnO particles on the surface of FAPs during the hydrothermal process. Accordingly, FAPs played an important role in the growth of ZnO precursor. Thus, the unique clustered shapes of ZnO on FAPs were formed to greatly increase the total surface area and are a potential photocatalyst suitable for the removal of pollutants.

Table 1. The comparison of surface areas of different samples using BET and the Langmuir equation

Materials	BET ( $\text{m}^2/\text{g}$ )	Langmuir ( $\text{m}^2/\text{g}$ )
Raw FAPs	2.38	2.95
Pristine ZnO	6.08	9.76
ZnO/FAPs - 50 mg	27.28	32.99
ZnO/FAPs - 100 mg	30.89	37.57

To investigate the photocatalytic performance of ZnO doped on FAPs, the experimental evaluation was carried out using MB dye. The photocatalytic evaluation of pristine ZnO and the different composite samples was based on the degradation of MB dye under constant UV irradiation in the same manner as in our previous report [31]. Figure 7 showed the experimental effect of ZnO doping on the surface of FAPs for the degradation of MB. After the 180 min experiment, the photodegradation of MB in the sample solution was compared to the level of control MB (10 ppm), pristine ZnO, and ZnO/FAPs (NM-3), as shown in Fig. 7. The comparison

revealed that the photodegradation efficiency of ZnO/FAP composites was more effective and was greatly enhanced by the incorporation of ZnO and FAPs compared to that of pristine ZnO. The analysis of NM-2 and NM-3 (Figs. 7b-c) showed that higher amounts of FAPs produced more enhanced photocatalytic property. The superior photocatalytic performance of the composite (NM-3) was related to the greater deposition of ZnO on the surface of FAPs and the electron transfer between the conduction bands of light-activated ZnO and light-activated FAPs [28].

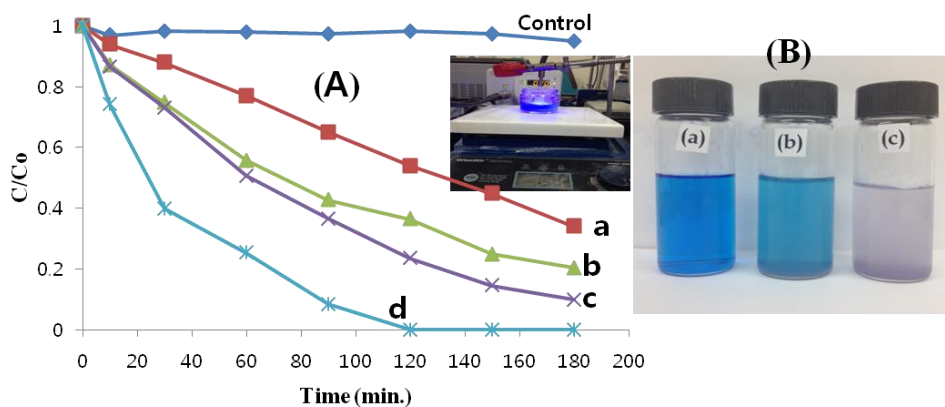


Fig. 7. (A) Comparison of the MB photodegradation of (a) pristine ZnO, (b) ZnO/FAPs 20 mg, (c) ZnO/FAPs 50 mg, and (d) ZnO/FAPs 100 mg. Inset (B) shows photographs of (a) control MB (10 ppm), (b) pristine ZnO, and (c) ZnO/FAPs 100 mg in solution after 180 min.

Photodegradation efficiency is affected by many factors such as material morphology, size, and structure, in addition to the manufacturing process and the properties of combined composites. As shown in Figs. 2b-c, the clusters of ZnO/FAP nanostructures were highly spherical and so produced high specific surface areas and were uniformly incorporated by the reaction in the hydrothermal process. Therefore, the morphology of the ZnO/FAP composite is sufficient to produce highly photocatalytic effects as a potential alternative material for the degradation of pollutants.

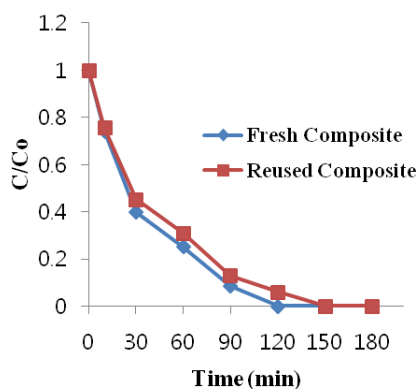


Fig. 8. Repeated evaluation (MB) of ZnO/FAP composite to demonstrate reusability.

This study included a recycling experiment that showed that the used composite materials can be reused with comparable photocatalytic activity. The experimental evaluation of the NM-3 composite was repeatedly performed to demonstrate its reusability. The result revealed that the composite has slightly lower efficiency compared to that in the initial evaluation. However, it showed the same general tendency and was considered as a valuable photocatalytic source.

#### 4. Conclusions

This study showed that the ZnO/FAP composite, possessing a highly effective photocatalytic property with highly adsorbent FAPs, was able to successfully produce photodegradation of MB and can be applied as an inexpensive and highly effective alternative catalyst for the removal of environmental pollutants. The formation of ZnO/FAP composite using hydrothermal fabrication in a facile process was demonstrated to result in the desired photocatalytic effect. Different amounts of FAPs (20, 50, and 100 mg) were blended in synthesized ZnO solution using a hydrothermal process. The morphology and characterization of the samples were analyzed by FE-SEM, EDS, TEM, XRD, FT-IR, PL, and BET measurements. The results showed that the photocatalytic efficiency of ZnO/FAP composites was greatly enhanced compared to that of pristine ZnO due to highly increased surface areas with unique cluster-shaped ZnO aspects on FAPs. Therefore, the as-synthesized composite can be used as an economical and environmentally friendly photocatalytic filler material in pollution-reduction applications.

#### Acknowledgements

This research was supported by research funds of Chonbuk National University in 2014 and by grants from the Korean Ministry of Education, Science and Technology (MEST) through the National Research Foundation (NRF) (Project no 2014-009068 and 2013-04015484). We would also like to thank Center for University Research Facility (CURF), Chonbuk National University for FE-SEM.

#### References

- [1] P.S. Suchithra, L. Vazhayal, A.P. Mohamed, S. Ananthakumar, *M Chem Eng J* **200**, 589 (2012) .
- [2] J.M. Herrmann, C. Guillard, P. Pichat, *Catal Today* **17** (1–2), 7 (1993).
- [3] S. Zheng, Y. Cai, K.E. O'Shea, *A: Chemistry* **210** (1), 61 (2010) .
- [4] K. Yeole, P. Kadam, S. Mhaske, *S Journal of Materials Research and Technology* **3**(2), 186 (2014).
- [5] P.K. Rohatgi, J.K. Kim, N. Gupta, S. Alaraj, A. Daoud, *Composites Part A: Applied Science and Manufacturing* **37**(3), 430 (2006) -437.
- [6] L.Q. Jing, D.J. Wang, B.Q. Wang, S.D. Li, B.F. Xin, H.G. Fu, J.Z. Sun, *J Mol Catal a-Chem* **244**(1-2), 193 (2006).
- [7] J.G. Yu, S.W. Liu, H.G. Yu, *J Catal* **249**(1), 59 (2007).
- [8] D.C. Reynolds, D.C. Look, B. Jogai, J.E. Hoelscher, R.E. Sherriff, M.T. Harris, M.J. Callahan, *J Appl Phys* **88**(4), 2152 (2000).
- [9] B. Swarnalatha, Y. Anjaneyulu, *Journal of Molecular Catalysis A: Chemical* **223**(1–2), 161 (2004) -165.
- [10] M.J. Height, S.E. Pratsinis, O. Mekasuwandumrong, P. Praserthdam, *Appl Catal B-Environ* **63**(3-4), 305 (2006).
- [11] C.C. Chen, *J Mol Catal a-Chem* **264**(1-2), 82 (2007).
- [12] N. Daneshvar, M. Rabbani, N. Modirshahla, M.A. Behnajady, *J Photoch Photobio A* **168**(1-2), 39 (2004).
- [13] C.X. Li, P.W. Huo, S.T. Li, Y.S. Yan, *Int J Mater Prod Tec* **39** (3-4), 330 (2010) .
- [14] P.W. Huo, Y.S. Yan, S.T. Li, H.M. Li, W.H. Huang, *Desalination* **256**(1-3), 196 (2010).
- [15] H.R. Pant, C.H. Park, P. Pokharel, L.D. Tijjing, D.S. Lee, C.S. Kim, *Powder Technol* **235** (0), 853 (2013).
- [16] K.I. Bolotin, K.J. Sikes, Z. Jiang, M. Klima, G. Fudenberg, J. Hone, P. Kim, H.L. Stormer, *Solid State Commun* **146** (9-10), 351 (2008).

- [17] P.S. Suchithra, C.P. Shadiya, A.P. Mohamed, P. Velusamy, S. Ananthakumar, *Applied Catalysis B: Environmental* **130–131** (0), 44 (2013) .
- [18] P. Huo, Z. Lu, X. Liu, D. Wu, X. Liu, J. Pan, X. Gao, W. Guo, H. Li, Y. Yan, *Chem Eng J* **189–190** (0), 75 (2012) -83.
- [19] A. Mercier, C. Joulain, C. Michel, P. Auger, S. Coulon, L. Amalric, C. Morlay, F. Battaglia-Brunet, *Water Res* **59** (0), 304 (2014).
- [20] J.C. Chai, K. Onitsuk, S. Hayashi, *J Hazard Mater* **166** (1), 67 (2009) -73.
- [21] D.P. Bentz, A.S. Hansen, J.M. Guynn, , *Cement and Concrete Composites* **33**(8), 824 (2011) .
- [22] J. Lu, F. Xu, D. Wang, J. Huang, W. Cai, *TJ Hazard Mater* **165**(1–3), 120 (2009).
- [23] W. Liu, X.-q. Shen, D.-h. Li, *Powder Technol* **186** (3), 273 (2008) -277.
- [24] C. Alkan, M. Arslan, C. Mehmet, M. Kaya, M. Aksoy, *Resour Conserv Recy* **13**(3-4), 147 (1995) .
- [25] A. Telesca, M. Marroccoli, C. D., V.G. L., M. F., *Waste Management* **33**(3), 628 (2013).
- [26] Q. Li, J. Pang, B. Wang, D. Tao, X. Xu, L. Sun, J. Zhai, *Adv Powder Technol* **24**(1), 288 (2013).
- [27] D.Y. Godovski, *Adv Polym Sci* 119, 79 (1995).
- [28] H.R. Pant, C.H. Park, B. Pant, L.D. Tijing, H.Y. Kim, C.S. Kim, *Ceram Int* **38**(4), 2943 (2012).
- [29] Y.H. Jiang, Y.M. Sun, H. Liu, F.H. Zhu, H.B. Yin, *Dyes Pigments* **78** (1), 77 (2008).
- [30] Q. Li , J. Pang, B. Wang, D. Tao, X. Xu, L. Sun, J. Zhai, *Advanced Power Technology* **24**(1), 288 (2013).
- [31] H.R. Pant, B. Pant, R.K. Sharma, A. Amarjargal, H.J. Kim, C.H. Park, L.D. Tijing, C.S. Kim, *Ceram Int* **39**(2), 1503 (2013).
- [32] J.G. Yu, H.G. Yu, B. Cheng, X.J. Zhao, J.C. Yu, W.K. Ho, *J Phys Chem B* **107**(50), 13871 (2003).
- [33] J. Yang, J. Zheng, H. Zhai, X. Yang, L. Yang, Y. Liu, J. Lang, M. Gao, *J Alloy Compd* **489**(1), 51 (2010).
- [34] H.Y. Yang, S.F. Yu, S.P. Lau, X.W. Zhang, D.D. Sun, G. Jun, *Small* **5**(20), 2260 (2009).